THE ASTROPHYSICAL JOURNAL, 366:328–339, 1991 January 1


# MAGNETOATMOSPHERIC OSCILLATIONS IN SUNSPOT UMBRAE

S. S. HASAN
Indian Institute of Astrophysics, Bangalore, India
*Received 1989 December 11; accepted 1990 June 26*

## ABSTRACT

Magnetoatmospheric oscillations in the umbra of a typical sunspot are investigated. Using a stratification in the umbral atmosphere, based upon the semi-empirical model of Maltby and coworkers, and assuming a vertical homogeneous magnetic field, the normal eigenfrequencies are numerically determined for various values of the horizontal wavenumber $k$ and displayed in the form of a diagnostic diagram. The results indicate the existence of several modes with periods in the 3 minute range. Furthermore, the analysis also demonstrates that waves in the 5 minute range can be resonant modes of the umbra itself, if the spot is deep enough. A noteworthy feature of the solutions is the existence of "avoided crossings," similar to those found in global oscillations. Apart from frequencies, eigenfunctions are also calculated, which allows the distribution of kinetic energy density and polarization with height to be analyzed. It is found that many modes have dominant kinetic energy in the photosphere, although there are also modes with appreciable energy in the chromosphere as well. In general, it is not possible to classify the modes in terms of the elementary modes of a homogeneous atmosphere. For large $k$, the modes resemble slow waves. However, for low values of $k$, corresponding to observed umbral oscillations, a simple global classification is not possible. The oscillations in the low photosphere and below are either fast-like or of the mixed kind, but above the temperature minimum they tend to acquire a slow or acoustic character. Finally, a comparison is made with other theoretical models of umbral oscillations.

*Subject headings:* hydromagnetics — Sun: atmosphere — Sun: magnetic fields — Sun: oscillations

## I. INTRODUCTION

After the discovery of umbral flashes by Beckers and Tallant (1969), numerous observations have confirmed the existence of oscillations in the umbrae of sunspots (see reviews by Moore 1981, Moore and Rabin 1985, and Thomas 1985 for references). The most commonly observed oscillations have periods typically in the range 120–200 s and occur over a height range extending from the photosphere to the transition region. Umbral oscillations in the aforementioned period range were observed in photospheric lines by Beckers and Schulz (1972), Giovanelli (1972), Bhatnagar and Tanaka (1972), Rice and Gaizauskas (1973), Thomas, Cram, and Nye (1984), Balthasar and Wiehr (1984), Lites and Thomas (1985), Abdelatif, Lites, and Thomas (1984, 1986); in chromospheric lines by von Uexküll, Kneer, and Mattig (1983), Lites (1984, 1986), and Gurman (1987); and in transition region lines by Gurman *et al.* (1982). Furthermore, there are also simultaneous observations of such oscillations in all three regions (Thomas *et al.* 1987).

In addition, oscillations with larger periods around 300–400 s are also observed in the photosphere (Bhatnagar, Livingston, and Harvey 1972; Giovanelli, Harvey, and Livingston 1978; Soltau, Schröter, and Wöhl 1976; Thomas, Cram, and Nye 1982, 1984; Balthasar, Küveler, and Wiehr 1987). There is, however, no indication for the presence of such oscillations in the chromosphere and transition region (Thomas *et al.* 1987).

A number of theoretical investigations have been carried out to explain umbral oscillations. Models for the 3 minute (hereafter referring to the range 120–200 s) oscillations fall into two broad categories. In the first model, the oscillations are interpreted essentially as trapped fast modes in the photosphere, which are driven by overstable convection in the subphotospheric layers (Uchida and Sakurai 1975; Antia and Chitre 1979; Scheuer and Thomas 1981; Thomas and Scheuer 1982). Tunneling upward along the field lines allows the oscillations to penetrate into the chromosphere, where they resemble acoustic waves (Thomas 1984). The waves suffer strong reflection in the transition region, though some leakage of wave energy into the corona also occurs (Scheuer and Thomas 1981; Schwartz and Leroy 1982). The alternative model proposed by Žugžda, Staude, and Locans (1983, hereafter ZLS) and by Gurman and Leibacher (1984) involves the excitation of a slow-mode resonance in the chromosphere by broad-band acoustic noise, impinging on the atmosphere from below. This "white" noise produces transmission peaks at a number of discrete frequencies, which are identifed with umbral oscillations. The latter are mainly confined to a cavity bounded from below by the temperature minimum and from above by the transition region.

Both models have their attractive features. As pointed out by Lites (1984, 1986), the existence of a number of closely spaced peaks in the 3 minute range are a natural consequence of the chromospheric resonance model, whereas in the detailed theory of Thomas and Scheuer (1982, hereafter TS), this feature does not appear to be present. On the other hand, the observation that the dominant energy of the oscillations is confined to the photosphere supports the photospheric resonance model of TS. Since the full set of equations are solved by TS, it appears that the difference between the two models, from a mathematical point of view, is basically related to different boundary conditions, particularly the location of the lower boundary. Otherwise, it is hard to understand how the resonances in the two models can be different, since, for a particular set of boundary conditions and horizontal wavenumber (assuming homogeneous conditions in the horizontal direction), the normal modes of oscillation of the umbral atmosphere are uniquely determined. The resonances occur at the normal-mode frequencies of the atmosphere. As regards the interpretation of the observed waves, it is misleading to distinguish

between the TS and ZLS models on the basis that in the former the resonance is a fast mode, whereas in the latter it is a slow mode. Indeed, as correctly pointed out by Thomas (1984), both fast- and slow-mode oscillations are present in the TS model. This is because a fast mode, excited in the subphotospheric layers, changes character as it propagates upward owing to the change in the ratio of the sound speed to the Alfvén speed with height. In the chromosphere this mode becomes converted into a slow mode. Thus, both the TS and ZLS models agree on the interpretation that in chromospheric layers and above, the mode is essentially an acoustic wave. The main disagreement between the two models is on the character of the modes in the photosphere.

As regards the interpretation of the 5 minute oscillations in sunspot umbrae, Thomas, Cram, and Nye (1982) have argued that these are driven by external $p$-modes. On the other hand, Žugžda (1984) has pointed out that these oscillations could be resonant modes of the spot itself. However, this hypothesis remains to be demonstrated quantitatively.

The purpose of the present investigation is to try to resolve some of the discrepancies between the two models and also to shed further light on the properties of umbral oscillations. We adopt the spirit of the TS calculation and determine the free eigenmodes of a model umbra. There are, however, two major differences between our respective calculations: first, we do not vary the location of the lower boundary to seek agreement with observation; second, we examine the behavior of the oscillation frequencies with horizontal wavenumber $k$, i.e., we generate a diagnostic diagram. The calculations of TS, which yield a single mode in the 3 minute range, were made for a fixed value of $k$. On the other hand, the ZLS model, which is capable of producing a number of modes in the observed range, is based upon the approximation of a strong magnetic field and large $k$. In this limit there is no dependence of the solutions on $k$. The results of the present analysis provide a more general range of solutions by examining the variation of frequency with $k$. As we shall see, this behavior reveals certain very interesting properties. A positive feature of the present work is that it demonstrates the existence of several modes in the 3 minute range, with dominant kinetic energy in the photosphere. Another new aspect of the analysis is an attempt to study the nature of the modes by decomposing them into solenoidal and irrotational parts.

The present investigation is a continuation of earlier work on wave propagation in thick flux tubes. In a previous analysis, using a rather simplified model for the umbra, Hasan and Abdelatif (1989) determined its oscillation spectrum and examined some properties of the modes. They found that there were several modes in the 3 minute range. The calculations were generalized by Hasan and Sobouti (1989), to use a model atmosphere for the umbra. However, for numerical reasons it was only possible to treat a fairly small vertical extension of the atmosphere. These difficulties have now been overcome by making substantial modifications in the mathematical technique, so that the sharp temperature rise, both in the chromosphere and in the convection zone, can be accommodated in the mathematical treatment.

The plan of the paper is as follows: In § II an empirical atmosphere for a sunspot umbra is described, which provides the starting equilibrium model for the linear analysis. The linearized equations are presented, followed by the method of solution in § IV. In § V the results of the calculations are presented, followed by a discussion in § VI. The application of the results to umbral oscillations is taken up in § VII, and a comparison with the TS and ZSL models is made in § VIII. Finally, a summary of the main findings and conclusions is presented in § IX.

## II. MODEL ATMOSPHERE FOR A SUNSPOT UMBRA

In order to compute the wave modes in an umbra, an equilibrium model is required, which mimics a real atmosphere in a sunspot. Recently, an umbral model was published by Maltby *et al.* (1986), which is an improvement on the reference model atmosphere of Avrett (1981) for the deeper layers below the photosphere. The chromospheric and higher portions in the atmosphere are based upon the model of Lites and Skumanich (1982) and Nicolas *et al.* (1981), respectively. Maltby *et al.* (1986) provide a model for an "average" umbral core (model M in their nomenclature). This model was extended beneath the photosphere by matching it smoothly with the convection zone model of Spruit (1977) (the combined model was kindly provided by T. Abdelatif). Figure 1 shows the temperature variation with $z$ (height) in a sunspot. The convention used is that $z$ increases away from the Sun, and $z = 0$ corresponds to optical depth unity.

Since the density $\rho$ and pressure $p$ are also tabulated in the model of Maltby *et al.* (1986), the mean molecular weight $\mu$ can be determined by using the perfect gas law relation

$$p = \frac{\rho \mathscr{R} T}{\mu}, \tag{1}$$

where $\mathscr{R}$ is the gas constant. Once the values of $T$ and $\mu$ are known, the pressure is recalculated using the equation of hydrostatic equilibrium,

$$\frac{dp}{dz} = -\rho g, \tag{2}$$

where $g$ is the acceleration due to gravity. The integration of equation (2) is carried out from $z = 0$ in both the upward and downward directions. The density is determined once again, using the perfect gas law.

## III. LINEARIZED EQUATIONS

The treatment in this section is closely parallel to the one found in Hasan and Sobouti (1987, hereafter Paper I). However, for the sake of completeness and also since there are

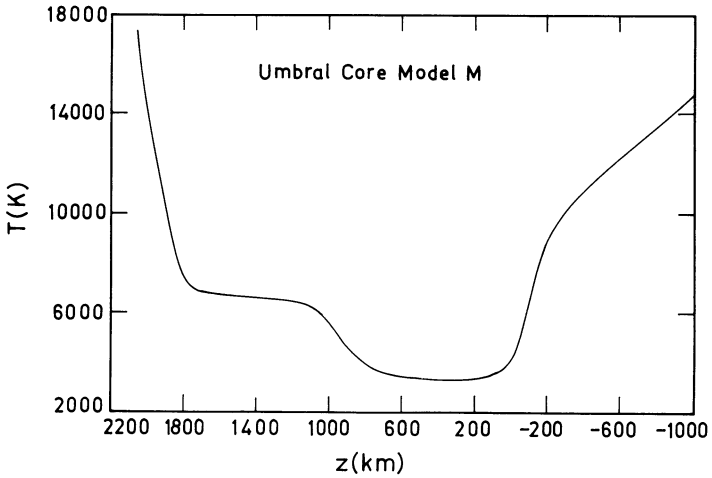


FIG. 1.—Temperature as a function of $z$ in a sunspot umbra (based upon the core umbral model M of Maltby *et al.* 1986).

several important differences, we present the complete set of equations. We assume that a uniform vertical magnetic field, of strength $B$, is embedded in the model atmosphere, described in the previous section. The normal modes can be determined by linearizing the magnetohydrodynamic (MHD) equations, which results in the following wave equation:

$$\rho \frac{\partial^2 \boldsymbol{\xi}}{\partial t^2} = -\boldsymbol{F}(\xi) , \tag{3}$$

where

$$\boldsymbol{F}(\xi) = \nabla \delta p - \boldsymbol{g}\, \delta\rho - \frac{1}{4\pi} (\nabla \times \delta \boldsymbol{B}) \times \boldsymbol{B} , \tag{4}$$

$$\delta\rho = -\rho \nabla \cdot \boldsymbol{\xi} - \boldsymbol{\xi} \cdot \nabla \rho , \tag{5}$$

$$\delta p = -\gamma p \nabla \cdot \boldsymbol{\xi} - \boldsymbol{\xi} \cdot \nabla p , \tag{6}$$

$$\delta \boldsymbol{B} = \nabla \times (\boldsymbol{\xi} \times \boldsymbol{B}) , \tag{7}$$

$$\boldsymbol{v} = \frac{\partial \boldsymbol{\xi}}{\partial t} , \tag{8}$$

where $\delta\rho$, $\delta p$, $\delta \boldsymbol{B}$ denote Eulerian perturbations in density, pressure, and magnetic field, respectively; $\boldsymbol{\xi}$ is a small Lagrangian displacement of a fluid element; $\boldsymbol{v}$ is the velocity; and $\gamma$ is the ratio of specific heats. On multiplying equation (3) by $\boldsymbol{\xi}^*$ and intergrating over the volume of the umbra, it is possible to show that (Paper I)

$$w - \omega^2 q = 0 , \tag{9}$$

where

$$\begin{aligned} w &= \int d\boldsymbol{x}\, \boldsymbol{\xi}^* \cdot \boldsymbol{F}(\boldsymbol{\xi}) \\ &= \int d\boldsymbol{x} \left( \frac{\delta p^* \delta p}{\rho c_s^2} + \rho N_g^2 \xi_z^* \xi_z + \frac{\delta \boldsymbol{B}^* \cdot \delta \boldsymbol{B}}{4\pi} \right) \\ &\quad + \int dA \left[ (\boldsymbol{n} \cdot \boldsymbol{\xi}^*) \delta p + \frac{1}{4\pi} (\boldsymbol{n} \cdot \boldsymbol{\xi}^*)(\boldsymbol{B} \cdot \delta \boldsymbol{B}) \right. \\ &\quad \left. - \frac{1}{4\pi} (\boldsymbol{B} \cdot \boldsymbol{n})(\boldsymbol{\xi}^* \cdot \delta \boldsymbol{B}) \right] , \end{aligned} \tag{10}$$

$$q = \int d\boldsymbol{x}\, \boldsymbol{\xi}^* \cdot \boldsymbol{\xi} , \tag{11}$$

$$N_g^2 = g \left( -\frac{1}{\rho} \frac{d\rho}{dz} - \frac{g}{c_s^2} \right) . \tag{12}$$

In deriving equation (10), we have assumed $\boldsymbol{\xi}$ to have a time dependence of the form $e^{-i\omega t}$. The second term, which represents a surface integral, arises due to integration by parts. We denote by $\boldsymbol{n}$ the unit outward normal vector from the surface, by $c_s = (\gamma p/\rho)^{1/2}$ the sound speed, and by $N_g$ the Brunt-Väisälä frequency. We shall consider only those perturbations for which the surface integral vanishes. The volume integrals are symmetric with respect to $\boldsymbol{\xi}$ and $\boldsymbol{\xi}^*$, from which it follows that $\omega^2$ is real.

## IV. METHOD OF SOLUTION

### a) *Decomposition of Displacements*

It is useful to decompose the displacements $\boldsymbol{\xi}$ into irrotational and solenoidal components using Helmholtz's theorem. A similar analysis, based upon such a decomposition for the linear displacements, was adopted by Aizenman and Smeyers (1977) and Sobouti (1981) in the context of global oscillations, and by Hasan and Sobouti (1987) for flux-tube oscillations. In the present case, the standard Helmholtz decomposition is used without the weighting factor $1/\rho$ used in Paper I.

Thus, according to Helmholtz's theorem, $\boldsymbol{\xi}$ can be broken up as follows

$$\boldsymbol{\xi} = \boldsymbol{\xi}_l + \boldsymbol{\xi}_t + \boldsymbol{\xi}_a , \tag{13}$$

where the various components can be expressed in terms of scalar functions $\phi_l$, $\phi_t$, and $\phi_a$ as follows:

$$\boldsymbol{\xi}_l = -\nabla \phi_l , \tag{14a}$$

$$\boldsymbol{\xi}_t = \nabla \times \nabla (z \phi_t) , \tag{14b}$$

$$\boldsymbol{\xi}_a = \nabla \times \nabla \times \nabla (z \phi_a) , \tag{14c}$$

where $z$ is a unit vector in the $z$-direction. It is instructive to rewrite equation (13) as

$$\boldsymbol{\xi} = \boldsymbol{\xi}_{\rm mag} + \boldsymbol{\xi}_a , \tag{15}$$

where

$$\boldsymbol{\xi}_{\rm mag} = \boldsymbol{\xi}_l + \boldsymbol{\xi}_t . \tag{16}$$

It can be shown (Paper I), that $\boldsymbol{\xi}_a$ and $\boldsymbol{\xi}_{\rm mag}$ describe Alfvén and magnetoatmospheric (MAG) waves, respectively. In fact, the equations for these modes become decoupled. We shall, in the present investigation, concern ourselves solely with MAG waves, deferring the solutions for Alfvén waves to another paper. Henceforth, only displacements of the type $\boldsymbol{\xi}_{\rm mag}$ will be considered (the subscript "mag" will hereafter be dropped).

### b) *Form of the Displacements*

Let $\boldsymbol{\zeta}$ denote a small displacement of a fluid element (note that $\boldsymbol{\zeta}$ need not satisfy eq. [9]). It is convenient to work in cylindrical coordinates $(r, \theta, z)$ and choose $\boldsymbol{\zeta}$ as follows

$$\zeta_r^o = -C_m \hat{\zeta}_r^o(z) \frac{dJ_m(kr)}{dr} e^{im\theta} , \tag{17}$$

$$\zeta_\theta^o = -C_m \frac{im}{r} \hat{\zeta}_\theta^o(z) J_m(kr) e^{im\theta} , \tag{18}$$

$$\zeta_z^o = -C_m ik \hat{\zeta}_z^o(z) J_m(kr) e^{im\theta} , \tag{19}$$

where $J_m$ denotes the Bessel function of order $m$, $k$ is the radial wavenumber, $C_m$ is an arbitrary constant, and the superscript $o$ is an integer characterizing the vertical order of the mode. A time dependence of the form $e^{-i\omega t}$ is implicit in equations (17)–(19). Let us consider purely axisymmetric modes, for which $m = 0$. Then $\zeta_\theta = 0$, and we have

$$\zeta_r = C_0 k \hat{\zeta}_r(z) J_1(kr) , \tag{20}$$

$$\zeta_z = -C_0 ik \hat{\zeta}_z J_0(kr) , \tag{21}$$

where the superscript $o$ has been dropped. It is convenient to choose

$$C_0 = \frac{1}{\sqrt{\pi} k a J_0(ka)} .$$

Following TS, let us assume that a sunspot umbra can be treated as a cylinder of radius $a$ and that the radial component of the displacement vanishes at $r = a$. Then, $k$ can take on only

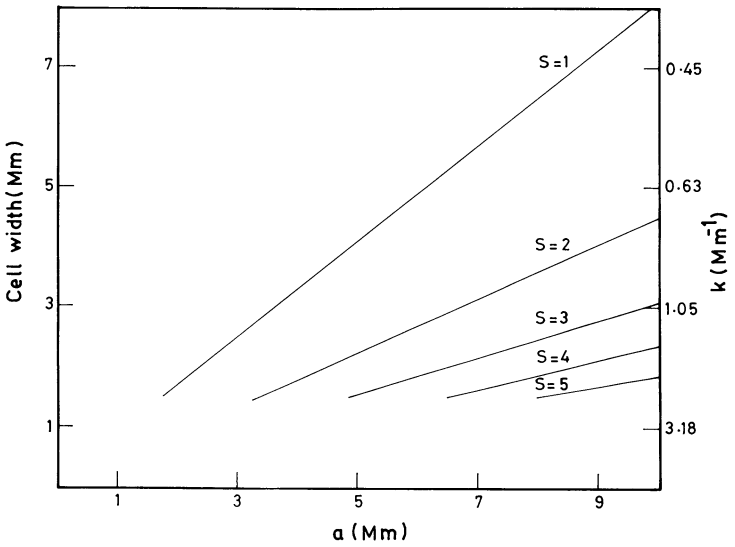


FIG. 2.—Cell width ($\lambda/2$) and horizontal wavenumber $k$ (on the right-hand axis) as a function of the umbral radius $a$, for axisymmetric modes having a node at $r = a$. The numbers denote the various order zeros of $J_1$.

discrete values, which are given by

$$ka = j_{1,s}\,, \quad (s = 1, 2, \ldots)\,, \tag{22}$$

where $j_{1,s}$ denotes the zero of order $s$ of $J_1$. Let us define a horizontal wavelength $\lambda$ associated with the horizontal displacements by the relation $\lambda = 2\pi/k$. Then $\lambda/2$ can crudely be regarded as the width of a vertical element in the umbra. Figure 2 shows the cell width ($\lambda/2$) and $k$ as a function of umbral radius $a$ for various $s$. Since the horizontal sizes are typically greater than 1.5 Mm, the curves have not been extended below this value. For instance, when $s = 1$ (which corresponds to the first zero of $J_1$), and $a = 4.2$ Mm, we find from Figure 2 that $k = 0.9$ Mm$^{-1}$. This value was used by Uchida and Sakurai (1975) and TS.

We also need to specify the form of $\hat{\zeta}_r$ and $\hat{\zeta}_z$. In principle any choice of functions which form a complete set, and which also satisfy the boundary conditions, can be used. The precise forms used in the present calculation are given in Appendix A.

### c) *Variational Method*

We now solve equation (9), using a variational technique. The method essentially consists of expanding $\boldsymbol{\xi}$ in terms of the trial functions $\boldsymbol{\zeta}$ as follows

$$\xi_r = \sum_o Z_r^o \zeta_r^o\,, \tag{23}$$

$$\xi_z = \sum_o Z_z^o \zeta_z^o\,, \tag{24}$$

where $Z_r^o$ and $Z_z^o$ are referred to as the variational constants. Substituting equations (23)–(24) in equation (9), and using a variational method to minimize the eigenvalues, yields a matrix equation of the form (Sobouti 1977; see also Paper I)

$$\boldsymbol{WZ} = \boldsymbol{SEZ}\,, \tag{25}$$

where $\boldsymbol{E}$ is a diagonal matrix whose elements are the eigenvalues $\omega^2$, and $\boldsymbol{Z} = [Z_i]$ $(i = r, z)$ is a column vector containing the variational constants. The elements of $\boldsymbol{W}$ and $\boldsymbol{S}$ are

$$W_{ij} = W_{ij}(1) + W_{ij}(2) + W_{ij}(3)\,, \tag{26}$$

where

$$W_{ij}(1) = \int dx\, \frac{\delta p_i^*\, \delta p_j}{\rho c_s^2}\,, \tag{27}$$

$$W_{ij}(2) = \delta_{iz}\delta_{jz} \int dx\, \rho N_g^2\, \zeta_z^*\, \zeta_z\,, \tag{28}$$

$$W_{ij}(3) = \int dx\, \frac{\delta \boldsymbol{B}_i^* \cdot \delta \boldsymbol{B}_j}{4\pi}\,, \tag{29}$$

and

$$S_{ij} = \int dx\, \rho \zeta_i^* \zeta_j\,, \tag{30}$$

where $\delta p$ and $\delta \boldsymbol{B}$ are given by equations (6) and (7) with $\boldsymbol{\xi}$ replaced by $\boldsymbol{\zeta}$ and $i, j = r, z$. The structure of the matrices $\boldsymbol{S}$ and $\boldsymbol{W}$ is given in Appendices B and C, respectively.

The matrix of eigenvalues is by definition block diagonal, with the following form:

$$\boldsymbol{E} = \begin{pmatrix} E_r & 0 \\ 0 & E_z \end{pmatrix}, \tag{31}$$

where each block is itself a diagonal matrix. The column vector $\boldsymbol{Z}$ has the structure

$$\boldsymbol{Z} = \begin{pmatrix} Z_r \\ Z_z \end{pmatrix}. \tag{32}$$

### d) *Boundary Conditions in the Vertical Direction*

In order to find a unique set of solutions, we need to impose boundary conditions. For the horizontal direction, we have assumed that the radial component of the Lagrangian displacement vanishes. Let us now consider the vertical direction. Following TS, we impose rigid boundary conditions,

$$\xi_r = \xi_z = 0 \quad \text{at} \quad z = h_- \quad \text{and} \quad z = h_+\,, \tag{33}$$

where $h_+$ and $h_-$ denote the top and bottom boundaries, respectively. Since it is not *a priori* obvious where these boundaries should be located, one must appeal to physical intuition to choose suitable levels. For $h_+$, TS argue that an appropriate height is at the chromosphere-coronal transition region, because, at this level, both the Alfvén and sound speeds are very large, thus leading to downward reflection of waves propagating from below. In the present calculation, it was found that the choice $h_+ = 2000$ km sufficed, since raising it any higher barely changed the frequency spectrum.

The choice of the lower boundary proved to be more difficult. TS adjusted this level to find modes with periods in the range 140–185 s. This level turned out to be some hundred kilometers below the surface for $B = 2000$ G. Physically, this procedure was justified on the basis that forcing by overstable convection would occur in a very narrow range of depths (according to Uchida and Sakurai 1975, when $v_A^2/c_s^2 \sim 1$), which are not very different from the values of $h_-$ found by TS. However, the assumption of overstability being confined to a very small layer may not be true (see § VIc), so that forcing would occur over a much larger range of depths. An alternative way to proceed might be to choose the lower boundary sufficiently deep that the oscillation frequencies, at least in the observed range, are somewhat insensitive to its precise location. Assuming that $h_-$ lies in the layers where $v_A/c_s < 1$, an asymptotic analysis of the equations (Žugžda 1984) reveals the

existence of basically two magnetoatmospheric modes. The first mode is essentially an acoustic mode, which on propagating downward will suffer upward reflection owing to the rapid increase of $c_s$ with depth. The other mode is essentially a gravity-modified slow wave, which for vertical propagation is mainly transverse ($\xi_z = 0$). Thus, the boundary conditions given by equation (33) can be physically justified for all modes, except for the horizontal displacement of the slow mode in the deep layers. The condition $\xi_r = 0$ at $z = h_-$ for this mode can, however, be crudely explained by arguing that the amplitudes of the motions in the deeper layers is likely to be small, owing to the large density of matter there. In the present calculation, the choice $h_- = -500$ km was selected iteratively.

### e) *Numerical Technique*

We have already seen that the integral formulation of the original wave equation finally reduces to the solution of equation (25). Details of the method can be found in Paper I. Briefly, the technique utilizes a Rayleigh-Ritz scheme to approximate the linear series by a finite number of terms, say $n$. The block matrices in $\boldsymbol{W}$ and $\boldsymbol{S}$ are of order $n \times n$. Equation (25) now reduces to a generalized eigenvalue problem, which can be solved using standard numerical algorithms.

## V. RESULTS

### a) *Diagnostic Diagram*

Figure 3 shows the variation of the wave frequency $\nu$ (where $\nu = \omega/2\pi$) with $k$ (diagnostic diagram) for umbral oscillations, for $B = 2000$ G (*solid lines*) and $B = 3000$ G (*dashed lines*). For a fixed value of $k$, a number of solutions exist satisfying the boundary conditions. These correspond to the normal-mode frequencies or harmonics, which form a discrete spectrum. The various numbers beside the solid curves denote the order $n$ of the solution for $B = 2000$ G. An interesting feature that can be discerned from the diagnostic diagram is the absence of accidental degeneracy in the solutions of different orders. It is found that when curves of adjacent orders draw close to one another, an "avoided crossing" occurs. Physically, this phenomenon is related to coupling between modes confined to different regions of the atmosphere (Leibacher and Stein 1981). Although "avoided crossings" have been extensively investigated in global oscillation studies (e.g. Osaki 1975; Aizenman and Smeyers 1977; Christensen-Dalsgaard 1980), their existence in the connection of magnetoatmospheric waves appears to have been noticed only recently (Hasan and Abdelatif 1989).

In an atmosphere, where the ratio of the sound to the Alfvén speed changes over several orders of magnitude, caution is needed when interpreting the waves in terms of the elementary modes of a homogeneous atmosphere. The variable structure of the atmosphere results in mode transformation, which is particularly effective in layers where $\omega H/v_A \sim 1$ (Žugžda 1984), where $H$ is the scale height of the atmosphere. Table 1 gives the values of $v_A$, $c_s$ and $\eta$, where $\eta = \omega H/v_A$, at various $z$ for $B = 2000$ G and $\omega = 3.49$ rad s$^{-1}$ (corresponding to a period

TABLE 1

VALUES OF $c_s$, $v_A$, AND $\eta = \omega H/v_A$ FOR DIFFERENT $z$

| $z$ (km) | $c_s$ (km s$^{-1}$) | $v_A$ (km s$^{-1}$) | $\eta$ |
|---|---|---|---|
| −500..... | 10.42 | 2.81(4.21) | 3.84(2.56) |
| −300..... | 9.61 | 3.63(5.45) | 2.44(1.62) |
| −100..... | 8.24 | 4.55(5.45) | 1.16(0.77) |
| 0..... | 6.52 | 5.48(8.22) | 0.59(0.40) |
| 100..... | 5.87 | 9.13(13.70) | 0.29(0.19) |
| 300..... | 5.94 | 34.82(52.23) | 0.08(0.05) |

NOTE.—$H$ is the scale height and $\omega$ the frequency; $B = 2000$ G and a wave period of 180 s are assumed. Numbers in parentheses correspond to $B = 3000$ G.

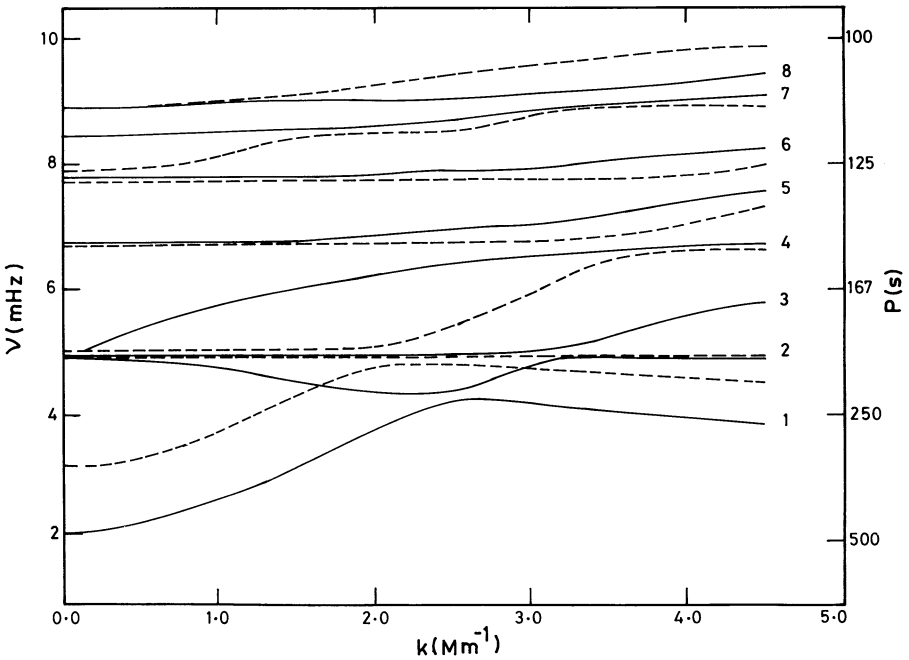


FIG. 3.—Variation of $\nu$ with $k$ in the umbra of a typical sunspot for $B = 2000$ G (*solid lines*) and $B = 3000$ G (*dashed lines*), corresponding to $v_{A0}/c_{s0} = 0.84$ and $v_{A0}/c_{s0} = 1.26$, respectively, where the subscript zero corresponds to $z = 0$. The right-hand scale denotes the periods, and the numbers beside the curves correspond to the order $n$ of the solution, with respect to $B = 2000$ G.

of 180 s). The numbers in parentheses give the values for $B = 3000$ G. We find that the "transformation" region occurs deeper in the umbra for $B = 3000$ G. Thus, when attributing a fast or slow character to a mode, it should be borne in mind that this is a local property, and applicable in layers separated from the "transformation region." Incidentally, decreasing the frequency moves this region lower down into the atmosphere.

Let us now see whether it is possible to extract any information on the nature of the models by looking at the diagnostic diagram, keeping the aforementioned points in mind. An examination of Figure 3 also shows that there are regions in the diagnostic diagram where the frequency hardly varies with $k$. These portions roughly correspond to modes which are dominantly of the slow type. In the upper layers of the atmosphere where $\eta \ll 1$, the slow-mode dispersion relation is

$$\omega \approx k_z c_s , \tag{34}$$

where $k_z$ is the vertical wavenumber. This relation shows that the slow mode is essentially an acoustic wave, whose frequency does not depend either on the horizontal wavenumber or on the magnetic field. In practice, we find that the situation is more complicated, owing to the fact that the modes also have nonnegligible energy in the lower layers, where the Alfvén and sound speeds are comparable, so that equation (34) is no longer valid. However, in the limit of large $k$, the dispersion relation for the slow mode is still given by equation (34), with $c_s$ replaced with $c_t$, where $c_t = c_s v_A/(c_s^2 + v_A^2)^{1/2}$. When $k \to \infty$, $\omega \to \infty$ for the fast mode, so that the two sets of modes are well separated in frequency. Thus, for large horizontal wavenumber, we expect the low-order modes to be of the slow type, whose frequencies depend on $B$ through the tube speed $c_t$. The magnetic nature of a mode can be seen by looking, in this limit, at the shift in frequency, when the magnetic field is varied. We find that the frequency of the $n = 2$ mode is unaffected by a change in the field, suggesting that this mode is dominantly acoustic in character. For the other modes, however, the frequency increases with $B$, although the dependence on field strength is fairly weak.

*b) Height Variation of the Velocity*

Figures 4*a* and 4*b* depict the variation of $v_z$ and $v_r$ with $z$ for $n \leq 5$, assuming $B = 2000$ G and $k = 0.9$ Mm$^{-1}$. Henceforth this choice of parameters will be used, unless stated otherwise. All amplitudes have been normalized with respect to the maximum over the vertical extension and essentially refer to the values on the axis of the flux tube. In order to compare the relative values of $v_r$ and $v_z$, the ratio $|v_r|_{max}/|v_z|_{max}$ is also given for each order $n$. We find that $|v_r|_{max} \ll |v_z|_{max}$, apart from the $n = 1$ mode, for which the two are comparable.

It is observed that, in general, at large heights the vertical and horizontal velocities increase and decrease, respectively, with $z$. This behavior can be understood by examining the asymptotic solutions of the equations of an isothermal atmosphere in the limit of small $\eta$, which have been discussed by Ferraro and Plumpton (1958). Above $z = 0$, the isothermal approximation is not very unreasonable, since $c_s$ does not change greatly. A decrease of $v_r$ with height, for large $z$, is due to the rapid increase of $v_A$ with $z$. On the other hand, $v_z$ increases with $z$ owing to the decline of density. The decrease in $v_z$, close to the upper boundary, occurs because of the sudden increase of $c_s$.

Table 2 shows the number of nodes in $v_r$ and $v_z$ for various

TABLE 2

NUMBER OF NODES IN $v_r$ AND $v_z$ FOR DIFFERENT ORDERS $n$[a]

| | Number of Nodes | |
|---|---|---|
| $n$ | $v_r$ | $v_z$ |
| 1..... | 0 | 1 |
| 2..... | 1 | 0 |
| 3..... | 1 | 1 |
| 4..... | 1 | 1 |
| 5..... | 1 | 2 |

[a] Assuming $B = 2000$ G and $k = 0.9$ Mm$^{-1}$.

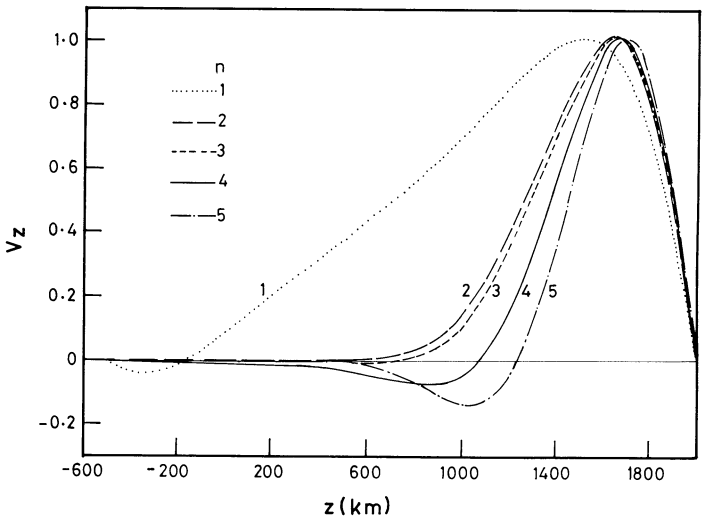


FIG. 4*a*

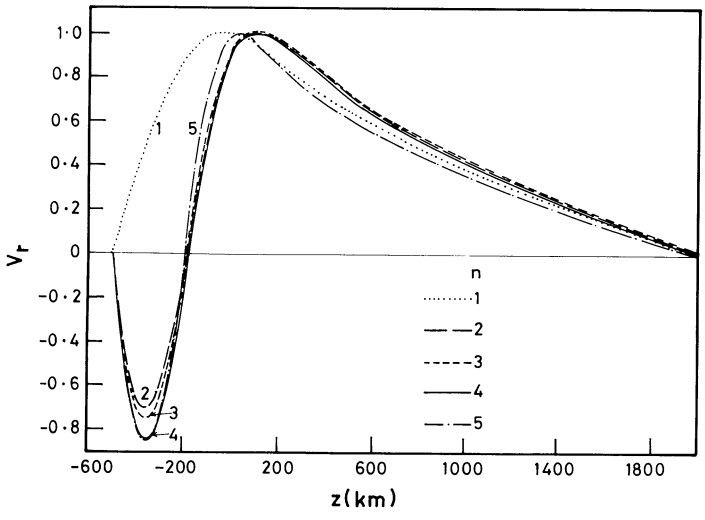


FIG. 4*b*

FIG. 4.—Variation with $z$ of (*a*) $v_z$ and (*b*) $v_r$ for $n = 1, 2, \ldots, 5$, assuming $B = 2000$ G and $k = 0.9$ Mm$^{-1}$. The values have been normalized with respect to the maximum in the interval. The ratios $|v_r|_{max}/|v_z|_{max}$ are 1.303, $3.845 \times 10^{-5}$, $3.111 \times 10^{-3}$, $3.585 \times 10^{-3}$, and $7.186 \times 10^{-5}$ for $n = 1, 2, \ldots, 5$, respectively.

orders. Apart from $n = 1$, the higher order curves have one node in $v_r$, which occurs at $z \approx -200$ km. It should be noted that classifying modes by the number of nodes in the horizontal and vertical velocities is not meaningful in the present case, because the problem under study is not of the standard Sturm-Liouville type.

*c) Height Variation of the Kinetic Energy Density*

It is interesting to examine the variation of the kinetic energy density with height in the various modes, particularly because of the observations of Abdelatif, Lites, and Thomas (1984) and Lites and Thomas (1985), which claim that the bulk energy of the 3 minute umbral oscillations is in the photosphere. Figure 5 shows the height variation of $E_{kin}$ [defined as $E_{kin} = \rho(v_r^2 + v_z^2)/2$] for $n \leq 5$. It may be observed that the energy of the modes is not spread uniformly over the height range under study, but rather confined to certain regions of the atmosphere. The $n = 1$ mode, for instance, appears to have negligible kinetic energy above a height of some 200 km, whereas the energy in the $n = 2$ mode is large in the upper part of the atmosphere. It can also be seen that for the $n = 3$ and $n = 4$ modes (corresponding to periods of 202 and 175 s), the dominant contribution to $E_{kin}$ comes from the photospheric and subphotospheric layers. Interestingly, the $n = 5$ mode (of period 150 s) has three peaks, which show that this mode has non-negligible energy over practically the full vertical extension of the atmosphere, with the largest contribution coming from the middle chromosphere. Although, in general $|v_z|_{max} \gg |v_r|_{max}$, with the maximum of $v_z$ occurring close to the top boundary, it should be borne in mind that the density is very low in the upper layers. In the photosphere and below, the main contribution to $E_{kin}$ is through $v_r$, since $v_z$ is fairly small. The occurrence of multiple peaks is due to the existence of nodes in the velocity distributions.

*d) Character of Displacements*

In § IVc, Helmholtz's theorem was used to decompose the linear displacements into longitudinal ($\xi_l$) and transverse ($\xi_t$) components. These are related to the scalar potentials $\phi_l$ and

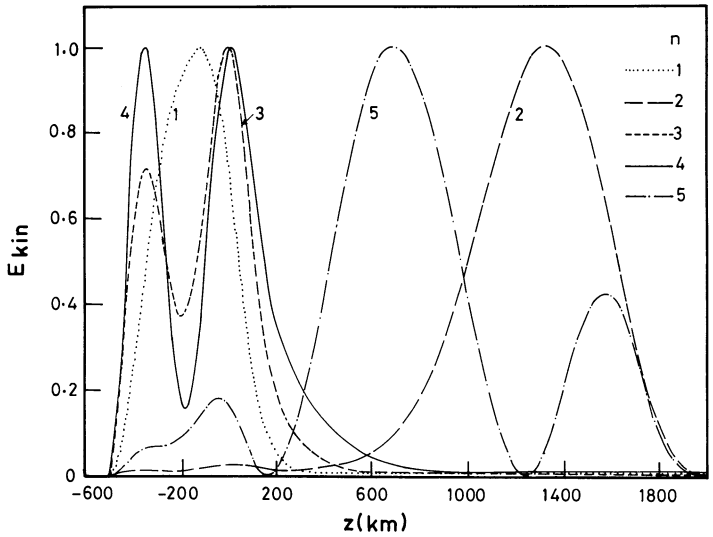


FIG. 5.—$E_{kin}$ vs. $z$ for $n = 1, 2, \ldots, 5$, assuming $B = 2000$ G and $k = 0.9$ Mm$^{-1}$. The values have been normalized with respect to the maximum in the interval.

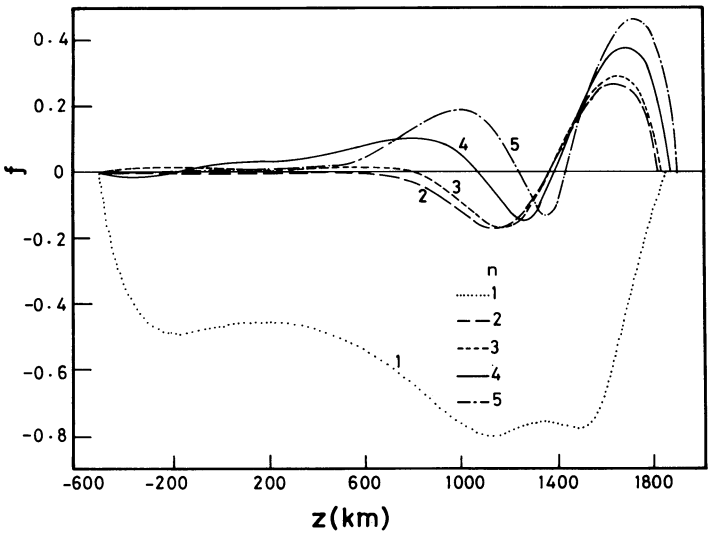


FIG. 6.—Variation of $f$ [$f = (|\xi_l| - |\xi_t|)/(|\xi_l| + |\xi_t|)$] with $z$ for $n = 1, 2, \ldots, 5$, assuming $B = 2000$ G and $k = 0.9$ Mm$^{-1}$.

$\phi_t$ through equations (14a) and (14b). In order to calculate $\phi_l$, let us take the divergence of equation (14a), which yields

$$\left(\frac{\partial^2}{\partial z^2} - k^2\right)\phi_l = -\nabla \cdot \xi \,. \tag{35}$$

Similarly, operating by $\nabla \times \nabla$ on equation (14b) yields the equation

$$\left(\frac{\partial^2}{\partial z^2} - k^2\right)\phi_t = -\frac{1}{k^2}(\nabla \times \nabla \times \xi)_z \,. \tag{36}$$

Equations (35) and (36) were solved, using standard techniques, to determine $\phi_l$ and $\phi_t$, from which $\xi_l$ and $\xi_t$ were determined using equations (14a) and (14b).

It is instructive to examine the "polarization" of a mode at different heights in the atmosphere. Similar to Hasan and Abdelatif (1989), let us define a quantity $f$, which is a measure of the longitudinal character of a mode, through the relation

$$f = \frac{|\xi_l| - |\xi_t|}{|\xi_l| + |\xi_t|} \,.$$

Thus, purely longitudinal and purely transverse modes correspond to $f = 1$ and $f = -1$, respectively. Figure 6 depicts the variation of $f$ with $z$. Let us first consider the $n = 1$ mode. This mode is transverse over the full vertical extension of the tube. For the $n > 1$ modes, the situation is not so unambiguous. These modes have comparable longitudinal and transverse components in the lower part of the atmosphere. However, with an increase in height, the modes tend to become predominantly longitudinal, with $f$ increasing with $n$.

Let us now see whether the aforementioned classification has a physical relationship with the fast and slow modes of a homogeneous medium. The $n = 1$ mode has significant energy in regions for which $z < 200$ km. In the region $0 < z < 200$ km (where $\eta < 1$), the magnetohydrodynamic (MHD) mode that is transverse is the fast one. For the other modes, it is not possible to establish a similar connection in the lower layers of the atmosphere. However, higher up in the atmosphere, these modes, which are predominantly longitudinal, have approximately a slow or acoustic character.

It should be pointed out that the simpler method of comparing the vertical and horizontal velocities for determining the polarization of a mode is not particularly useful in the present context, since the direction of propagation of a wave changes with height owing to the variable sound and Alfvén speeds.

## VI. DISCUSSION

### a) General Comments

The results presented in the previous section have highlighted several interesting features of wave propagation in the umbral atmosphere. We have found that the oscillation spectrum covers a broad range of frequencies. Modes with fairly close frequencies can have very different properties. The nature of a mode can also change with horizontal wavenumber and result in "avoided crossings," between different order solutions. The distribution of the kinetic energy density (in the oscillations) exhibits peaks, which occur at different locations for the various order modes. A global interpretation of the solutions in terms of elementary MHD modes is not applicable, owing to the sharp variation of $\eta$ with height. However, in certain limits a rough correspondence can be established, in a local sense, in layers which are separated from the "transformation region."

In the previous section it was stated that in the limit of large horizontal wavenumber, the lower order modes are of the slow type. The assumption that is implicit here is that the magnetic field is sufficiently large to suppress the instability arising due to the superadiabatic temperature gradient in the convection zone. However, if the sunspot is sufficiently deep, then instability in the form of overturning convection can occur. The most unstable mode is one with large $k$ and physically corresponds to an almost incompressible displacement which produces negligible deformation of the field. Indeed, Moreno Insertis and Spruit (1989) found that a spot with a field of 3000 G, extending to some 5000 km below the surface, is unstable to convection. They calculated a growth time of about 18 minutes, with the maximum of the vertical velocity amplitude occurring at a depth of some 2300 km. However, observations suggest that spots, at least in the surface layers and above, are stable. Thus, either convective instability does not occur or, if it does, then it produces very little effect in the observable layers. The instability can be suppressed by the field (2000–3000 G) of the spot, if the latter does not extend too deep. At present, it is difficult to distinguish between these possibilities. However, even if convective modes are absent, the presence of thermal diffusion gives rise to an overstable form of instability, which persists even when $B \to \infty$ (Syrovatskii and Žugžda 1968). We shall return to this point later when the mechanism of mode excitation is discussed.

### b) Sensitivity of the Results to $h_-$

It was mentioned in § IV that the results are not senstive to the location of the upper boundary, if it is placed sufficiently high. However, the choice of the lower boundary is more difficult to select. Although some heuristic arguments were given to justify the choice $h_- = -500$ km, it would be interesting to see how the results would be modified when a different value of $h_-$ is used. Table 3 gives the frequencies (periods in parentheses) of various order modes for $h_- = -500$, $-2000$, and $-160$ km, for $B = 2000$ G and $k = 0.9$ Mm$^{-1}$. The ordering of the modes is with respect to $h_- = -500$ km. In the case $h_- = -2000$ km, there are also modes (not tabulated) with periods larger than

TABLE 3

FREQUENCIES AND PERIODS OF VARIOUS ORDER MODES FOR DIFFERENT LEVELS OF LOWER BOUNDARY

| | $\nu$ (MHz) | | |
|---|---|---|---|
| $n$ | $h_- = -500$ km | $h_- = -2000$ km | $h_- = -160$ km |
| 1..... | 2.59(387) | 2.12(461) | ... |
| | ... | 2.61(383) | ... |
| | ... | 3.12(320) | ... |
| | ... | 3.33(300) | ... |
| | ... | 3.38(296) | ... |
| | ... | 3.86(259) | ... |
| 2..... | 4.79(209) | 4.78(209) | 4.79(209) |
| 3..... | 4.95(202) | 4.80(208) | ... |
| 4..... | 5.71(175) | 5.59(179) | 5.82(172) |
| | ... | 6.34(158) | 6.44(155) |
| 5..... | 6.66(150) | 6.54(153) | ... |
| | ... | ... | 7.12(140) |
| 6..... | 7.75(129) | 7.12(140) | ... |

NOTE.—Periods are given in parentheses. $B = 2000$ G and $k = 0.9$ Mm$^{-1}$ are assumed. The ordering is with respect to $h_- = -500$ km.

$P_1$ (where the subscript denotes the mode order), with bulk energy below the subphotosphere. A comparison of the three sets of values shows fairly close agreement, apart from the $n = 1$ mode. The insensitivity of the periods of the $n \geq 2$ modes to the position of $h_-$ is, possibly, a consequence of the fact that these modes have very small amplitudes in the deep layers below the surface. However, the situation is different for the $n = 1$ mode, whose frequency is decreased, owing to the larger distance over which the mode has significant amplitude. It should be borne in mind that increasing the depth of the lower boundary to $-2000$ km also introduces extra modes, such as those with periods between $P_1$ and $P_2$. There are also intermediate modes—for example, those with periods near $P_5$. The close frequencies of the two modes get resolved when the lower boundary is sufficiently deep. For similar reasons the mode corresponding to $n = 3$ is absent when $h_- = -160$ km. It thus appears that the periods of the modes in the 3 minute range are somewhat independent of $h_-$, so long as it is located far from the "transformation" region.

### c) Mode Excitation

Although we do not consider the question of mode excitation in the present analysis, it is still worthwhile to comment briefly on it. As discussed in § VI*b*, it is possible to have overstable oscillations excited in the superadiabatic layer below $z = 0$. The possibility of overstable oscillations in sunspots was first examined by Danielson (1961), based on the treatment of Chandrasekhar (1961). This mechanism has subsequently been extensively investigated using linear theory (Danielson 1965; Musman 1967; Savage 1969; Syrovatskii and Žugžda 1968; Žugžda 1971; Moore 1973; Mullan and Yun 1973; Anita and Chitre 1979). The overstable mode is essentially a slow wave constrained to move along the field. Approximate calculations of Moore (1973) and Mullan and Yun (1973) indicate that waves with periods in the observed range can be excited by oscillatory convection. However, these analyses were made in the Boussinesq approximation and should be viewed with caution. Regarding the extension of the overstable region, Meyer *et al.* (1974) calculated a value of some 2000 km (below $z = 0$) by considering the relative values of thermal and magnetic diffusiv-

ities. There are at present no quantitative calculations of the periods and eigenfunctions of overstable modes for a sunspot stratification. It would be desirable to have these, in order to ascertain whether there are overstable oscillations in the observed range of frequencies in the umbral atmosphere.

The other possibility is the suggestion of ZSL, according to which mode excitation occurs through selective transmission of a broad-band spectrum of acoustic waves, incident at the lower boundary of the spot. In this picture, the upward-propagating waves undergo mode conversion in the "transformation zone." A physical description of the processes occurring in this zone has been given by Žugžda (1984). Essentially, the upward-transmitted wave flux consists of both fast and slow modes. In addition, there is a downward-reflected slow mode. Standing modes are set up owing to wave reflections, as already described. The umbral atmosphere essentially acts as a filter in which the transmitted spectrum has peaks at the resonant frequencies.

On the basis of the present model, it is difficult to choose between the two processes, since our calculations do not rely on any specific excitation mechanism. A theory for umbral oscillations, in which the mode excitation mechanism is incorporated in a self-consistent manner, could possibly throw light on this question. However, this would involve nonlinear calculations, which are beyond the scope of this investigation.

## VII. UMBRAL OSCILLATIONS

### *a) Oscillations in the 3 Minute Range*

Let us first consider the application of the results to 3 minute oscillations. As already pointed out, these actually refer to oscillations with periods in the range 120–200 s. From Table 3 we find that there are several modes with periods in the observed range. For example, Thomas, Cram, and Nye (1984) found peaks in the power spectrum at periods of 197, 171, and 155 s, which correspond to the modes ($P_2/P_3$), $P_4$, and $P_5$. The close frequencies of the $n = 2$ and $n = 3$ modes will probably show up as a single mode in the observations. Table 4 gives the frequencies of the modes observed by Gurman (1987) in active regions AR 4598 and AR 4629, using the chromospheric line Mg II K, formed near the temperature minimum. A comparison of these frequencies with modes of order 4, 5, and 6 in the present calculation again shows reasonable agreement.

### *b) Oscillations in the 5 Minute Range*

We also find that there are normal modes of the umbra, which falls in the 5 minute range. From Table 3 one discerns the presence of several modes with periods in the range 250–500 s (for $h_- = -2000$ km). For $h_- = -500$ km, only a single period in this range is present, and when $h_- = -160$ km, there are no modes in the 5 minute range. Thus, the deeper the spot, the denser is the spectrum of modes. However, increasing the depth below 2000 km produces minor changes in the spectrum in the aforementioned range. Despite the uncertainties of the present model, let us compare the periods (for $h_- = -2000$ km) with the observations of Thomas, Cram, and Nye (1984). The photospheric power spectrum obtained by them exhibited peaks at periods of 366, 301, 270, and 197 s. It is somewhat fortuitous that these periods agree fairly well with those calculated here. Even if the agreement is coincidental, the present model does, however, demonstrate that oscillations with periods near 5 minutes can also be resonant modes of the sunspot itself, unless the latter is very shallow.

TABLE 4

FREQUENCIES OF UMBRAL OSCILLATIONS OBSERVED BY GURMAN 1987[a]

| FREQUENCY (mHz) | |
|---|---|
| AR 4598 | AR 4629 |
| 5.49 | 5.29 |
| 6.46 | 6.42 |
| 7.43 | 7.55 |

[a] Using the Mg II K line.

## VIII. COMPARISON WITH THE TS AND ZSL MODELS

The spirit of the present calculation is very similar to the one adopted by TS. Essentially, the main difference between our papers is the location of the lower boundary, apart from the equilibrium atmosphere model for the umbra. This fact should be borne in mind when comparing the results of the two models. In the TS model, the lower boundary is taken to be some hundred kilometers deep (e.g., $h_- = -153.4$ km corresponds to a period of 185 s, for $B = 2000$ G and $k = 0.9$ $Mm^{-1}$), which is justified on the grounds that it is precisely in these layers that forcing by overstable convection occurs. We have seen that the assumption of overstability existing only in a very narrow range of depths may not be valid. This does not, however, rule out mode excitation by overstability; rather, it implies that the question of the depths over which it occurs has to be examined carefully. The TS calculations reveal the presence of only a single mode (for fixed $k$) in the 3 minute range. On the other hand, we find that there are multiple modes with frequencies in the 3 minute range, which are not greatly sensitive to the exact location of the lower boundary. Many of the modes have large kinetic energy density in the photosphere, which is in agreement with the TS model and the observations of Abdelatif, Lites, and Thomas (1984) and Lites and Thomas (1985). The two models, however, disagree on the interpretation of 5 minute oscillations. According to the TS model, there are no normal modes in this range. In the present investigation, we find that, if the spot is sufficiently deep, there can also be resonant modes in this range. The possibility of 5 minute oscillations from the external photosphere penetrating into the umbra, as suggested by Thomas (1982) (see also Thomas, Cram, and Nye 1982; Abdelatif 1985), cannot be entirely discounted, although the observations of Balthasar, Küveler, and Wiehr (1987) cast some doubt on this.

The ZSL model essentially involves calculating the resonance periods at which the transmission coefficient of wave energy through the photosphere and chromosphere has a maximum, for a broad-band acoustic flux incident from below. These calculations were made under the strong-field assumption (i.e., $v_A/c_s \gg 1$), valid only in the upper photosphere and above. The transmission of acoustic waves is calculated for waves, incident from below, at a boundary in this region. The model provides a reasonable representation for the chromospheric resonances, but is not accurate for treating modes, which have large energy in the lower layers. Another approximation inherent in the ZSL model is the limit $k \to \infty$, which removes any $k$ dependence and effectively eliminates the fast mode. From the diagnostic diagram (Fig. 3), we find that for certain modes the frequency does not vary strongly with $k$, so

that this limit can give an approximate estimate of these frequencies. However, the physical nature of the modes can depend sensitively on $k$. For instance, Hasan and Abdelatif (1989) find that the behavior of the eigenfunctions, the kinetic energy density distribution, and the polarization of the modes change with $k$. The kinetic energy density in the ZSL model, in general, appears to be larger in the chromosphere than in the photosphere, whereas we find that this is not always true. It is not possible to compare the phase relationships published by ZSL, since we have not made any allowance for wave leakage at the upper boundary. Regarding the 5 minute oscillations, Žugžda (1984) points out that these can be present in a subphotospheric cavity in the ZSL model, which is in qualitative agreement with the findings of the present analysis.

## IX. SUMMARY AND CONCLUSIONS

The main purpose of the present investigation was to focus, in a quantitative way, on the nature of umbral oscillations. A realistic model for the sunspot stratification was used, based upon a published empirical model atmosphere. Approximating the sunspot as a thick flux tube of circular cross section, the axisymmetric normal modes of MAG waves were determined and a diagnostic diagram was generated for different field strengths. A noteworthy feature that could be discerned from this diagram was the existence of avoided crossings in the solutions of MAG modes in a sunspot atmosphere. Eigenfunctions were also determined, from which the distribution of kinetic energy density could be examined. For many of the modes, $E_{\rm kin}$ is higher in the photosphere. But there are also modes for which $E_{\rm kin}$ can be high in the upper layers, or distributed over a large height range in the upper photosphere and lower chromosphere. By decomposing the displacements into transverse and longitudinal parts, the "polarization" of a mode could be studied as a function of height in the atmosphere. In the limit of large $k$, the low-order modes resemble slow waves. However, for low values of $k$ (corresponding to umbral oscillations) a global identification with the elementary MHD modes does not appear possible. In the photosphere and below, the modes are either fast-like or mixed, but in the chromosphere they acquire a slow or acoustic character.

An application of the results to 3 minute oscillations showed that the multiple peaks in the observed power spectrum could be roughly identified with the computed normal modes. These results were not found to be sensitive to the precise location of the lower boundary. The theoretical analysis also indicated that oscillations in the 5 minute range can be resonant modes of the umbra.

A positive feature of the present analyses (like that of TS) is that it solves the full system of equations, without the limitations inherent in the ZSL treatment. Our investigation, in principle, allows both photospheric and chromospheric resonances to be treated. The analysis does not rely upon any specific mechanism of mode excitation; it is compatible with both forcing by overstability and forcing by broad-band acoustic noise. Results of the calculations are in reasonable agreement with observations.

From a theoretical point of view, it is fairly encouraging to note that despite a number of uncertain parameters, the results compare favorably with observations. However, the model has scope for development. The adiabatic assumption and the neglect of leakage of wave energy at the upper boundary could be relaxed as a next step. Mathematically, this would make the eigenvalue problem non–self-adjoint and render the frequencies complex. It would be possible to determine phase relationships between various quantities, which could meaningfully be compared with observations. Another feature which eventually should be incorporated in a self-consistent way is the excitation mechanism. It is hoped that these refinements will be made in forthcoming investigations.

I am grateful to Y. Sobouti for the use of his subroutine package to solve generalized eigenvalue problems, to T. Abdelatif for providing an umbral atmospheric model, to J. Thomas and B. Roberts for discussions and helpful comments, and to M. H. Gokhale for kindly reading the manuscript.

## APPENDIX A

## FORMS OF THE TRIAL FUNCTIONS $\hat{\zeta}_r^o$ AND $\hat{\zeta}_z^o$

From equations (20) and (21), we have

$$\zeta_r^o = C_0 k \hat{\zeta}_r^o J_1(kr) ,$$
$$\zeta_z^o = -C_0 ik \hat{\zeta}_z^o J_0(kr) ,$$

where $C_0 = [\pi^{1/2} ka J_0(ka)]^{-1}$. Let us choose

$$\hat{\zeta}_z^o = -i \sqrt{\frac{\rho_0}{\rho}} \sin\left[\frac{o\pi(z - h_-)}{d}\right], \tag{A1}$$

where $d = h_+ - h_-$. Henceforth, the caret above $\zeta$ will be dropped. The function $\zeta_z$ satisfies the boundary conditions given by equation (33). Although a similar form for $\zeta_r$ could be used, it was found that, in practice, faster convergence was obtained by choosing $\zeta_r$ as a solution of the following equation:

$$\left(\frac{d^2}{dz^2} - k^2\right)\zeta_r^o = k\alpha^o(z) , \tag{A2}$$

where

$$\alpha^o(z) = -i\frac{c_s^2}{v_A^2}\left(\frac{d}{dz} - \frac{g}{c_s^2}\right)\zeta_z^o , \tag{A3}$$

subject to the boundary conditions given by equation (33). Equation (A2) can be derived from equation (3) in the limit $v_A/c_s \gg 1$.

It is easy to see that equation (A2) has the solution

$$\zeta_r^o = \frac{1}{\sinh kd}\left[\sinh k(h_+ - z)\int_{h_-}^{z} dz' \sinh k(z' - h_-)\alpha^o(z') + \sinh k(z - h_-)\int_{z}^{h_+} dz' \sinh k(h_+ - z)\alpha^o(z')\right]. \tag{A4}$$

## APPENDIX B

## MATRIX ELEMENTS OF $\boldsymbol{S}$

It is easy to see that $\boldsymbol{S}$ is block diagonal with the following structure:

$$\boldsymbol{S} = \begin{pmatrix} S_{rr} & 0 \\ 0 & S_{zz} \end{pmatrix}. \tag{B1}$$

Explicit expressions for the block elements of $\boldsymbol{S}$ are

$$S_{rr}^{oo'} = \int dz\, \rho\zeta_r^{o*}\zeta_r^{o'} , \tag{B2}$$

$$S_{zz}^{oo'} = \int dz\, \rho\zeta_z^{o*}\zeta_z^{o'} . \tag{B3}$$

The integrals in equations (B2) and (B3) can be evaluated numerically.

## APPENDIX C

## MATRIX ELEMENTS OF $\boldsymbol{W}$

The block structure of the $\boldsymbol{W}$ matrix is

$$\boldsymbol{W} = \begin{pmatrix} W_{rr}(1) + W_{rr}(3) & W_{rz}(1) \\ W_{zr}(1) & W_{zz}(1) + W_{zz}(2) \end{pmatrix}. \tag{C1}$$

Explicit expressions for the block elements of $\boldsymbol{W}$ are

$$W_{rr}^{oo'}(1) = k^2 \int dz\, \gamma p\zeta_r^{o*}\zeta_r^{o'} , \tag{C2}$$

$$W_{rz}^{oo'}(1) = -ki \int dz\, \gamma p\zeta_r^{o*}\left(\frac{d\zeta_z^{o'}}{dz} + \frac{p'}{\gamma p}\zeta_z^{o'}\right), \tag{C3}$$

$$W_{zz}^{oo'}(1) = \int dz\, \gamma p\left(\frac{d\zeta_z^{o*}}{dz} + \frac{p'}{\gamma p}\zeta_z^{o*}\right)\left(\frac{d\zeta_z^{o'}}{dz} + \frac{p'}{\gamma p}\zeta_z^{o'}\right), \tag{C4}$$

$$W_{zz}^{oo'}(2) = \int dz\, \rho N_g^2 \zeta_z^{o*}\zeta_z^{o'} , \tag{C5}$$

$$W_{rr}^{oo'}(3) = \frac{B^2}{4\pi}\int dz\left(\frac{d\zeta_r^{o*}}{dz}\frac{d\zeta_r^{o'}}{dz} + k^2\zeta_r^{o*}\zeta_r^{o'}\right). \tag{C6}$$

## REFERENCES


Abdelatif, T. E. 1985, Ph.D thesis, University of Rochester.
Abdelatif, T. E., Lites, B. W., and Thomas, J. H. 1984, in *Small-Scale Dynamical Processes in Solar and Stellar Atmospheres*, ed. S. L. Keil (Sunspot: Sacramento Peak Observatory), p. 141.
———. 1986, *Ap. J.*, **311**, 1015.
Aizenman, M. L., and Smeyers, P. 1977, *Ap. Space Sci.*, **48**, 123.
Antia, H., and Chitre, S. M. 1979, *Solar Phys.*, **63**, 67.
Avrett, E. H. 1981, in *The Physics of Sunspots*, ed. L. E. Cram and J. H. Thomas (Sunspot: Sacramento Peak Observatory), p. 235.
Balthasar, H., Küveler, G., and Wiehr, E. 1987, *Solar Phys.*, **112**, 39.

Balthasar, H., and Wiehr, E. 1984, *Solar Phys.*, **94**, 99.
Beckers, J. M., and Schulz, R. B. 1972, *Solar Phys.*, **27**, 61.
Beckers, J. M., and Tallant, P. E. 1969, *Solar Phys.*, **7**, 351.
Bhatnagar, A., Livingston, W. C., and Harvey, J. W. 1972, *Solar Phys.*, **27**, 80.
Bhatnagar, A., and Tanaka, K. 1972, *Solar Phys.*, **24**, 87.
Chandrasekhar, S. 1961, *Hydrodynamic and Hydromagnetic Stability* (Oxford: Clarendon).
Christensen-Dalsgaard, J. 1980, *M.N.R.A.S.*, **190**, 765.
Danielson, R. E. 1961, *Ap. J.*, **134**, 289.
———. 1965, in *IAU Symposium 22, Stellar and Solar Magnetic Fields*, ed. R. Lüst (Amsterdam: North-Holland), p. 314.
Ferraro, V. C., and Plumpton, C. 1958, *Ap. J.*, **129**, 459.
Giovanelli, R. G. 1972, *Solar Phys.*, **27**, 71.
Giovanelli, R. G., Harvey, J. W., and Livingston, W. C. 1978, *Solar Phys.*, **59**, 40.
Gurman, J. B. 1987, *Solar Phys.*, **108**, 61.
Gurman, J. B., and Leibacher, J. W. 1984, *Ap. J.*, **283**, 859.
Gurman, J. B., Leibacher, J. W., Shine, R. A., Woodgate, B. E., and Henze, W. 1982, *Ap. J.*, **253**, 939.
Hasan, S. S., and Abdelatif, T. 1989, in *Physics of Magnetic Flux Ropes*, ed. C. T. Russell and E. R. Priest (AGU Monog.), in press.
Hasan, S. S., and Sobouti, Y. 1987, *M.N.R.A.S.*, **228**, 427 (Paper I).
———. 1989, in *IAU Symposium 138, Solar Photosphere: Structure, Convection, and Magnetic Fields*, ed. J. O. Stenflo (Dordrecht: Kluwer), p. 255.
Leibacher, J. W., and Stein, R. F. 1981, in *The Sun as a Star*, ed. S. Jordan (Washington, DC: NASA), p. 263.
Lites, B. W. 1984, *Ap. J.*, **277**, 874.
———. 1986, *Ap. J.*, **301**, 939.
Lites, B. W., and Skumanich, A. 1982, *Ap. J. Suppl.*, **49**, 293.
Lites, B. W., and Thomas, J. H. 1985, *Ap. J.*, **294**, 682.
Maltby, P., Avrett, E. H., Carlsson, M., Kjeldseth-Moe, O., Kurucz, R. L., and Loeser, R. 1986, *Ap. J.*, **306**, 284.
Meyer, F., Schmidt, H., Weiss, N. O., and Wilson, P. R. 1974, *M.N.R.A.S.*, **169**, 35.
Moore, R. L. 1973, *Solar Phys.*, **30**, 403.
———. 1981, in *The Physics of Sunspots*, ed. L. E. Cram and J. H. Thomas (Sunspot: Sacramento Peak Observatory), p. 259.
Moore, R. L., and Rabin, D. 1985, *Ann. Rev. Astr. Ap.*, **23**, 239.
Moreno Insertis, F., and Spruit, H. C. 1989, *Ap. J.*, **342**, 1158.
Mullan, D. J., and Yun, H. S. 1973, *Solar Phys.*, **30**, 83.
Musman, S. 1967, *Ap. J.*, **149**, 201.
Nicholas, K. R., Kjeldseth-Moe, O., Bartoe, J.-D. F., and Bruekner, G. E. 1981, in *The Physics of Sunspots*, ed. L. E. Cram and J. H. Thomas (Sunspot: Sacramento Peak Observatory), p. 167.
Osaki, Y. 1975, *Pub. Astr. Soc. Japan*, **27**, 237.
Rice, J. B., and Gaizaukas, V. 1973, *Solar Phys.*, **32**, 421.
Savage, B. D. 1969, *Solar Phys.*, **156**, 707.
Scheuer, M. A., and Thomas, J. H. 1981, *Solar Phys.*, **71**, 21.
Schwartz, S., and Leroy, B. 1982, *Astr. Ap.*, **112**, 93.
Sobouti, Y. 1977, *Astr. Ap.*, **55**, 327.
———. 1981, *Astr. Ap.*, **100**, 319.
Soltau, D., Schröter, E. H., and Wöhl, H. 1976, *Astr. Ap.*, **50**, 367.
Spruit, H. 1977, Ph.D. thesis, University of Utrecht.
Syrovatskii, S. I., and Žugžda, Yu. D. 1968, *Soviet Astr.*, **11**, 945.
Thomas, J. H. 1982, *Ap. J.*, **262**, 760.
———. 1984, *Astr. Ap.*, **135**, 188.
———. 1985, *Australian J. Phys.*, **38**, 811.
Thomas, J. H., Cram, L. E., and Nye, A. H. 1982, *Nature*, **297**, 485.
———. 1984, *Ap. J.*, **285**, 368.
Thomas, J. H., Lites, B. W., Gurman, J. B., and Ladd, E. F. 1987, *Ap. J.*, **312**, 457.
Thomas, J. H., and Scheuer, M. A. 1982, *Solar Phys.*, **79**, 19 (TS).
Uchida, Y., and Sakurai, T. 1975, *Pub. Astr. Soc. Japan*, **27**, 259.
von Uexküll, M., Kneer, F., and Mattig, W. 1983, *Astr. Ap.*, **123**, 263.
Žugžda, Yu. D. 1971, *Cosmic Electrodynamics*, **2**, 267.
———. 1984, *M.N.R.A.S.*, **207**, 731.
Žugžda, Yu. D., Staude, J., and Locans, V. A. 1983, *Solar Phys.*, **82**, 369 (ZLS).

S. S. Hasan: Indian Institute of Astrophysics, Sarjapur Road, Bangalore 560 034, India